Dispersive excitation transport at elevated temperatures (50–298 K): Experiments and theory

Alan D. Stein, Kristen A. Peterson,[a] and M. D. Fayer
Department of Chemistry, Stanford University, Stanford, California 94305

(Received 27 November 1989; accepted 22 January 1990)

Time-resolved fluorescence depolarization has been used to measure electronic excitation transport among naphthyl chromophores in polymeric glasses. 2-ethylnaphthalene randomly distributed in PMMA and 2-vinylnaphthalene/methyl methacrylate copolymer in PMMA were studied. It was found that excitation transport is dispersive at all temperatures studied, from 50 K to room temperature, i.e., the extent of transfer depends on the excitation wavelength within the S_0–S_1 absorption band. A theory based on the nondispersive, Förster mechanism for excitation transfer has been developed to describe dispersive transport. Good agreement between the theoretical and experimental results are achieved without resorting to adjustable parameters. Both the theory and experiment show that, for the observable used here, excitation at a certain wavelength, called the "magic wavelength," results in a time dependence that is identical to the Förster nondispersive result, i.e., dispersive transport appears to vanish.

I. INTRODUCTION

The effect of the spatial distribution of molecules on the rate and extent of intermolecular electronic excitation transport in condensed phase systems has been the subject of numerous experimental and theoretical studies in recent years.[1] The development of accurate statistical mechanical theories to describe excitation transfer among chromophores has developed to the point where the time dependence of excitation transport can be quantitatively modeled for complicated spatial distributions of chromophores.[2–6] This makes it possible for experiments measuring intermolecular excitation transport to be used as probes of the spatial geometry of complex systems. Systems that have been studied by this technique include bilayers and multibilayers,[4] colloids[7] and micelles,[3] and polymer chains in liquid[8] and solid solutions (blends).[9,10] Useful quantitative information on a molecular distance scale has been measured by combining experimental results with theoretical calculations.

At or near room temperature the excitation transfer rate has been assumed to be independent of chromophore energy. For singlet excited states the distance dependence of the transfer rate is governed by a dipole–dipole interaction. The quantum mechanics of the energy transfer step is incorporated into a single pairwise, distance dependent transfer rate developed by Förster[11] to theoretically explain transfer between donors and acceptors in solution. In the Förster theory the transfer rate is expressed in terms of the spectral overlap of the emission spectrum of the donor and the absorption spectrum of the acceptor. The spectral lines of the chromophores are taken to be homogeneously broadened; thermal fluctuations in the solvent broaden the spectral lines to an extent which is much greater than the inhomogeneous linewidth. No explicit consideration of how thermal energy is absorbed or emitted by the chromophores in conserving energy during the transfer step is necessary. In the case of donor–donor transfer, excitation transfer between two chemically identical species, the Förster theory predicts symmetric forward and back transfer rates.

While electronic excitation transfer theories for room temperature systems have been developed for complicated chromophore geometries, other investigations have addressed the question of how energy inhomogeneity in an ensemble of chromophores at low temperature affects the rate of energy transport. Low temperature (4.2–120 K) experiments have shown that when an electronic transition is predominantly inhomogeneously broadened, excitation transfer becomes dispersive,[12–19] i.e., dependent on the excitation energy. Theories to explain this behavior have considered phonon assisted hopping[20–23] or a kinetic model with a rate constant for transfer which varies with time.[12,24] Monte Carlo simulations have been used to model systems in which an excitation makes many hops through a system of chromophores with a distribution of energies and distance scales.[25] However, the complications of including chromophore energies into the excitation transfer problem have limited these theoretical investigations to systems of simple chromophore distributions, such as random solutions and chromophores substituted in a crystal lattice.

Situations in which the inhomogeneous broadening is larger than the thermal, homogeneous broadening of spectral lines are generally assumed only to occur at low temperatures. There are, however, cases of inhomogeneous spectral broadening at high temperatures.[12] When inhomogeneous broadening is of the order or larger than homogeneous broadening the donor–donor pairwise transfer rate in the Förster theory is not symmetric because the spectral emission–absorption overlap between two chemically identical molecules depends on which molecule of the pair is initially excited. For a spatial distribution of chromophores with a distribution of electronic transition energies an excitation not only moves spatially among the chromophores, but it moves to lower energy as it is transferred. The excitation

[a] Present address: MS J567, Los Alamos National Laboratory, Los Alamos, NM. 87544.

 0021-9606/90/095622-14$03.00

will tend to move to the red edge of the absorption line by a series of transfer steps to lower energy chromophores while emitting phonons (heat) to conserve energy.

At low temperatures this has been observed by measuring spectral diffusion,[13-16,26] time-resolved exciton phosphorence,[12,17] the rate and extent of exciton trapping,[12] and the rate of carrier recombination.[18,19] In spectral diffusion experiments, excitations which originate near the absorption line center are seen to move to lower energy sites by measuring the fluorescence spectrum at various delay times. In the exciton hopping experiments and recombination experiments, the rate of trapping is dependent on the number of sites an exciton can sample. Measurements have shown that the hopping rate is time dependent due to evolution in time of the exciton to lower energy states. The trapping rate also depends on the initial point of excitation in the absorption line. The excitation energy dependence and time dependence of the rate of excitation transfer in these systems have led to the transport being termed dispersive.

Recently, we gave a brief report of the first observation of dispersive electronic excitation transport at and near room temperature by monitoring the time-resolved fluorescence depolarization from an ensemble of chromophores.[27] The systems studied were random copolymers of 2-vinylnaphthalene and methyl methacrylate dissolved in small concentration in bulk poly(methyl methacrylate). Measurements were made at a number of excitation wavelengths and sample temperatures. The sensitivity of this experimental technique to the details of the time dependence of excitation transfer made it possible to reveal the energy dependent transfer among chromophores for which the homogeneous and inhomogeneous linewidths are similar. A theory was developed to model the experimental results in terms of known quantities about this system. It was found that the experimental findings could be explained nearly quantitatively by modifying the theory of Peterson and Fayer,[5] for nondispersive excitation transfer among chromophores randomly attached to a polymer chain, with details of the spectral characteristics of the chromophores and assumptions about the mechanism of dispersive energy transfer.

The experiments have now been extended to include measurements of dispersive transport in a simpler system, 2-ethylnaphthalene (2-EN) molecules randomly distributed in PMMA. It was found that the free naphthyl chromophores have a different inhomogeneous linewidth than when attached to a polymer chain. The 2-EN in PMMA experiments show that dispersive energy transport at high temperatures can also be measured in a system with less inhomogeneous broadening. Theoretically, the geometrical constraints on energy transfer are more easily handled in this system than when the chromophores are attached to a polymer chain. It provides a simpler system for developing a theory to describe dispersive transport, which can then be applied to more complicated spatial distribution functions.

In this paper we will present the experimental findings on high temperature dispersive transport in both of these systems of chromophores dispersed in polymeric solids. Additionally, we will describe in detail the theory which mimics the experimental results. This theory contains no adjustable parameters. All of the necessary input parameters for the theory can be measured independently. This presentation will show why dispersive transport is occurring in these materials and how it affects the extent of energy transport measured experimentally.

It will also be demonstrated theoretically and experimentally that under the appropriate conditions, the influence of dispersive transport can be neglected and theories based on the conventional Förster transfer mechanism can be employed. This situation occurs for a special wavelength of initial excitation which we call the "magic wavelength."

II. EXPERIMENTAL PROCEDURES

A. Materials

Two types of solid polymeric solutions were used in this study. In the first, a 2-vinylnaphthalene/methyl methacrylate copolymer (2-VN/MMA) is dispersed in bulk poly(methyl methacrylate) (PMMA). The second solution is of randomly distributed 2-ethylynaphthalene (2-EN) in PMMA. As will be discussed further below, these samples differ in both the spatial and energetic distributions of the naphthyl chromophores.

Mixtures with two different copolymers were used in this study: (I) $M_w = 23\,000$, $M_w/M_n = 1.3$, with 9% vinylnaphthyl monomers; (II) $M_w \sim 50\,000$, with one or no vinylnaphthyl monomer per chain (no excitation transport). The copolymers were synthesized by a free radical mechanism following the method of Fox *et al.*[28] The percentage of naphthyl chromophores in the copolymer was determined by absorption spectroscopy. Gel permeation chromotography was used to determine the molecular weight and polydispersity of (I). A freeze-dried solution of a copolymer and PMMA was molded in a stainless-steel press above the glass transition temperature of PMMA ($T_g = 105$ °C). The preparation of the copolymers and solid blends with PMMA are described more thoroughly in Refs. 9 and 10.

The naphthyl units, pendant to the copolymer chain, are randomly distributed along the chain in relatively low concentration. Thus, in the case of copolymer (I) with 9% 2-VN monomers, there is no quasi-one-dimensional transport down the chain backbone. The copolymer is present in a low concentration in the host PMMA (0.38% by weight) such that no interchain transport occurs; all electronic excitation transport is three-dimensional among the chromophores attached to one chain. Describing energy transport in this system requires consideration of the finite volume and nonrandom distribution of chromophores.

In the second type of solution used in this study, 2-ethylnaphthalene randomly dispersed in PMMA, two different concentrations of 2-EN were used. One was so low that no intermolecular energy transfer could occur. The other contained enough chromophores (0.22 M 2-EN/PMMA) that a significant amount of excitation transfer occurred within two lifetimes of the 2-ethylnaphthyl first singlet excited state (~ 100 ns). Thin films of the polymer solutions were cast from 5%–10% solutions (by weight of polymer) in THF. The THF was removed by slow evaporation and then the samples remained under vacuum for many days. These sam-

ples were checked for excimer fluorescence, which would indicate that the 2-EN aggregated in the polymer, but none was detected. The optical densities of the samples are less than 0.1, to eliminate fluorescence reabsorption. Electronic energy transport in this system occurs among an infinite system of randomly distributed chromophores.

B. Optical measurements

Electronic excitation transport (EET) measurements were made by measuring polarized fluorescence using two methods, time-correlated single photon counting and measurement with a fast photodetector and a transient digitizer. The laser system and electronics associated with the transient digitizer data collection system have been described in detail previously.[9,10] Therefore, only the single photon counting system is described below. The results obtained from the two apparatus are the same. However, time-correlated single photon counting can provide better signal-to-noise ratios. This system replaced the transient digitizer system in the course of these experiments.

The ultraviolet light source used to excite the naphthyl chromophores is obtained by frequency doubling a tunable, cavity dumped dye laser. The home built dye laser is synchronously pumped by a Spectra-Physics model 3800 Nd:YAG laser which is frequency doubled to 532 nm. The cavity dumper (Spectra-Physics model 344) in the dye laser provides single pulse selection of the mode-locked pulses at 800 kHz. The pulse width of the dye laser run at red wavelengths (DCM as the laser dye) is typically 15 ps. The pulse energy is ~ 10 nJ. The dye laser output is frequency doubled using a KDP crystal. The conversion efficiency to the UV is $\sim 2\%$.

The wavelength of the ultraviolet excitation pulse is measured with a 3/4 m monochromator. The bandwidth of the laser is 0.1 nm. The wavelength of the excitation pulse is changed by adjusting a two-plate birefringent filter in the dye laser cavity.

The UV laser light is attenuated such that the observed fluorescence is at the single photon level (one photon is detected for every ~ 40 cavity dumped pulses). The single photons are detected by a photomultiplier tube (Hamamatsu R1527). The signal from the PMT is amplified, passed through a constant fraction discriminator, and is the stop pulse for a time to amplitude convertor. The start pulse is obtained from a fast photodiode (HP 5082-4220) which detects each cavity dumped dye laser pulse. The output of the time to amplitude convertor is processed and saved by a multichannel analyzer (Ortec-Norland 5600), and then passed to a computer.

Fluorescence depolarization spectroscopy is used to experimentally measure $r(t)$, the time-resolved fluorescence anisotropy. Fluorescence polarized parallel and perpendicular to the polarization of the excitation pulse is collected separately. The nonresonant fluorescence is detected through a monochromator with a 10 nm bandwidth to prevent scattered laser light from reaching the photomultiplier detector. A Pockels cell is used as an electro-optic half-wave plate to alternately polarize the excitation beam in perpendicular directions. A fixed polarizer is attached to the input slit of the monochromator; only light of one polarization passes through the monochromator. In this way the measured fluorescence intensity is independent of any bias of the monochromator or detector to light of either polarization.

The polarization of the excitation beam is changed at regular 20 s intervals. This time is chosen such that any long term intensity fluctuations in the laser power cannot cause a distortion in the relative amounts of the parallel and perpendicular fluorescence. A computer synchronizes the voltage applied to a Pockels cell, alternating back and forth between collecting parallel and perpendicular fluorescence, until a sufficient signal-to-noise ratio is reached. This procedure is repeated on various spots on the sample and the results are averaged. The polarization of the excitation beam passing through the sample is measured to insure that the sample has no birefringence which would distort the polarization of the fluorescence.

III. CALCULATING THE TIME DEPENDENCE OF EXCITATION TRANSPORT FROM THE EXPERIMENTAL MEASUREMENTS

The fluorescence anisotropy $r(t)$ is related to the fluorescence polarized parallel $[I_{\parallel}(t)]$ and perpendicular $[I_{\perp}(t)]$ to the excitation beam by

$$I_{\parallel}(t) = e^{-t/\tau}[1 + 2r(t)],$$

$$I_{\perp}(t) = e^{-t/\tau}[1 - r(t)]. \tag{1}$$

$r(t)$ is calculated from the parallel and perpendicular data,

$$r(t) = \frac{[I_{\parallel}(t) - I_{\perp}(t)]}{[I_{\parallel}(t) + 2I_{\perp}(t)]}. \tag{2}$$

Dividing by $I_{\parallel}(t) + 2I_{\perp}(t)$ in Eq. (2) gives $r(t)$ that is independent of the fluorescence lifetime or the functional form of the population decay. The fluorescence anisotropy includes contributions from all sources of depolarization; it decays in time as a result of chromophore motion and excitation transport. Chromophore motion leads to rotation of the transition dipole relative to the direction of excitation polarization. Excitation transport takes the initial excitation into the ensemble of other unexcited chromophores with random transition dipole directions. Subsequent emission results in fluorescence depolarization.[29]

On the time scale of the experiment, 1–100 ns, rotation of the chromophores is very slow. Therefore, it is accurate to assume that the anisotropy from all sources of depolarization is separable, i.e.,

$$r(t) = C \cdot G^{s}(t)\phi(t). \tag{3}$$

$\phi(t)$ is the decay of the time dependent anisotropy from rotational motion. $G^{s}(t)$ characterizes the rate of excitation transport. It is the probability that the initially excited chromophore is still excited at time t. It contains contributions from excitations which have never transferred and from excitations which have transferred away but then returned to the initially excited chromophore. It is a fundamental quantity in the theoretical description of excitation transport. C is the anisotropy from time independent sources of depolarization.

$G^{s}(t)$, the excitation transport observable, is obtained

by measuring $r(t)$ for two different samples. One solid solution (I) has chromophores present in a high local concentration and excitation transport takes place (chromophores are separated by distances of the order of R_0, the Förster radius). This is the main source of fluorescence depolarization. Another blend (II) is chemically identical to (I), but has chromophores present in such a low concentration that no excitation transport takes place. $G^s(t) = 1$ for all time. Fluorescence in (II) is depolarized due to rotation of the excited chromophore and the time-independent extent of polarization of the naphthyl electronic transition. $G^s(t)$ is obtained by dividing the anisotropies obtained from the two samples:

$$G^s(t) = r_{\mathrm{I}}(t)/r_{\mathrm{II}}(t). \tag{4}$$

IV. EXPERIMENTAL RESULTS

Table I gives the spectral characteristics of the S_0–S_1 electronic transition for the naphthyl chromophores in the two types of samples used in this study. The absorption spectra of the naphthyl chromophores were measured at temperatures from room temperature to 65 K by using a Hg arc lamp and the 3/4 m monochromator. None of the wavelengths reported here have been corrected for vacuum. The invariance of the linewidth on cooling the samples from 100 to 65 K leads us to assign the full width at half-maximum at 65 K to be the inhomogeneous linewidth. Figure 1 shows absorption spectra of 2-VN/MMA in PMMA at 65 K and 298 K. Shown in Table II is a comparison between the measured room temperature linewidths and linewidths calculated with the assumption that the absorption line at room temperature can be modeled as a Voigt profile, a convolution of a Lorentzian homogeneous line of width kT and a Gaussian inhomogeneous line of width equal to that measured at low temperatures. The Voigt linewidths and the measured room temperature linewidths are in reasonably good agreement, demonstrating that a Lorentzian homogeneous line and a Gaussian inhomogeneous line are good models for the chromophores in this system at the temperatures we are considering. Other studies[12,30] have shown the validity of modeling the shape of the inhomogeneous line in an amorphous system as a Gaussian.

An interesting observation from Table I is the difference in measured inhomogeneous linewidths for the naphthyl chromophores in the two systems studied here. The inhomogeneous linewidth is ~50% larger when the naphthyl unit is attached to the polymer chain than when it is free from this constraint. The inhomogeneous linewidth reflects the distribution of transition energies of the chromophores in the host. Glasses are known to cause broad inhomogeneous linewidths as compared to a crystal due to a greater extent of

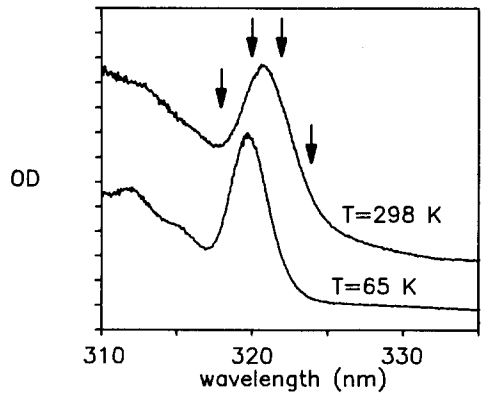

FIG. 1. Absorption spectra of naphthyl chromophores of a 2-VN/MMA copolymer dispersed in PMMA at room temperature ($T = 298$ K) and 65 K. The band near 320 nm (31 250 cm^{-1}) is due to excitations from the ground state to the S_1 electronic state. It is a shoulder on the much stronger S_0–S_2 absorption further to the UV. As the temperature is decreased from room temperature, the linewidths become narrower and the peak of the S_0–S_1 line appears to shift to the blue. We have assigned the center of the inhomogeneously broadened line to be 319.5 nm, and the inhomogeneous linewidth to be 300 cm^{-1} based on the spectrum taken at 65 K. The arrows point out excitation wavelengths of interest in this work: 318, 320, 322, and 324 nm.

disorder at the molecular level. The greater inhomogeneous linewidth for the polymer bound chromophores can imply a broader distribution of local environments. Attaching the chromophore to the polymer backbone reduces its ability to adjust to local molecular structures at the time of sample preparation. The unbound chromophore has greater freedom to sample distinct configurations in the local structure. This will enable it to find a deeper local minimum on the potential surface, and the ensemble will not have as broad a distribution of these local minima. The bound chromophore can have a greater tendency to be trapped in unfavorable configurations, resulting in a broader distribution of configurations, and a broader inhomogeneous line. The inhomogeneous linewidth of the 2-EN in PMMA system was measured for samples prepared by the solvent casting technique as well as by molding the polymer melt. Both preparations gave chromophores with the same inhomogeneous linewidth. This suggests that the method of preparation of these samples does not strongly influence the final distribution of local structures.

Time-resolved fluorescence depolarization measurements were made on both the solid solutions of tagged polymer (2-VN/MMA copolymer) in PMMA and the solid mixtures of free chromophore (2-EN) in PMMA. The experiment was performed on samples in which electronic excitation transport occurred, and on similar samples with a

TABLE I. Measured parameters of S_0–S_1 absorption line.

Sample	Inhomogeneous FWHM 298 K	Inhomogeneous FWHM 65 K	Line center
2-VN/MMA in PMMA	410 cm^{-1}	300 cm^{-1}	319.5 nm
2-EN in PMMA	360 cm^{-1}	215 cm^{-1}	318.0 nm

TABLE II. Comparison between measured and calculated FWHM at 298 K of S_0–S_1 absorptions.

Sample	FWHM 298 K Measured	FWHM 298 K Calculated
2-VN/MMA in PMMA	410 cm^{-1}	425 cm^{-1}
2-EN in PMMA	360 cm^{-1}	345 cm^{-1}

lower concentration of chromophores in which the only source of time-dependent fluorescence depolarization was due to chromophore reorientation. The fluorescence depolarization was measured at different excitation wavelengths in the origin of the S_0–S_1 electronic absorption of the naphthyl chromophores. The measurements were made at room temperature and at lower temperatures down to 50 K by mounting the samples in contact with the cold finger of a He closed cycle refrigerator.

From the fluorescence detected parallel and perpendicular to the excitation beam polarization, the fluorescence anisotropy as a function of time is obtained as described above. $G^s(t)$, the time-dependent probability that the originally excited chromophore is still excited at time t, is constructed from $r(t)$ measured for the two different concentration samples. Figure 2(a) shows the measurement of the extent of excitation transport that takes in place in a sample of 2-VN/MMA copolymer in PMMA at 100 K as the excitation wavelength is changed. For one wavelength, $G^s(t)$ decreases in time as a result of transfer of the excitation to surrounding chromophores, which reduces the probability that the initially excited chromophore is still excited. As the excitation wavelength is moved to longer wavelength (lower energy) the rate of energy transport decreases. This can be seen from the $G^s(t)$ curves. The slope of $G^s(t)$ gives the rate of transfer and the value at a given time is the probability that the excitation remains on the initially excited chromophore. Figure 2(b) shows the same measurement made on the same sample, but at room temperature (298 K). The extent of dispersive transport is decreased but can still be seen in this figure. This is the first observation of dispersive excitation transport at room temperature. It is made possible by the great sensitivity of the measurement of $G^s(t)$, by time-resolved depolarization, to the details of the rate of excitation transport.

Figure 3 displays $G^s(t)$ for the same sample measured with one excitation wavelength, 322 nm, at a number of temperatures. When the excitation is well to the red of the center of the electronic absorption line the rate and extent of excitation transport is strongly dependent on the sample temperature. At this excitation wavelength, electronic excitation transport occurs more slowly as the temperature is decreased because fewer chromophores are thermally accessible, effectively reducing the concentration.

Figure 4 shows the results of a similar experiment done on samples containing 2-EN randomly distributed in a PMMA glass. The line center of the origin of the first singlet absorption is shifted by roughly 1.5 nm to the blue in 2-EN as compared to when the naphthalene is attached to the polymer chain (Table I). It can be seen in Fig. 4(a) that at room temperature there is a small but visible change in $G^s(t)$ as the excitation wavelength is changed. Thus, dispersive transport is seen at room temperature in a system in which the inhomogeneous linewidth is approximately equal to kT, the thermal energy. When the temperature is lowered to 100 K the rate of excitation transport becomes strongly dependent on the excitation wavelength. This is exhibited in Fig. 4(b).

Dispersive transport has been observed and discussed extensively for low temperature systems, typically below 50 K. At low temperatures, particularly around the helium boiling point, homogeneous absorption lines are very narrow, and dispersive transport can be readily observed by time-dependent shifting and broadening of the fluorescence or phosphorescence spectrum. Very broad absorption and

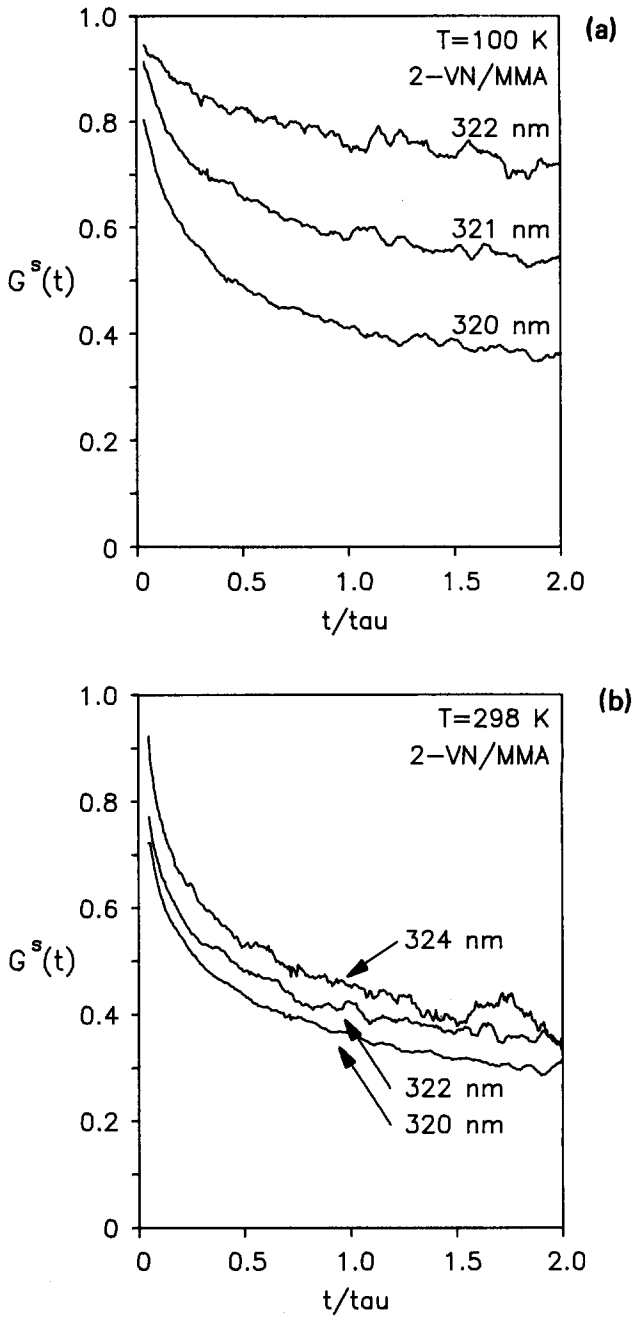

FIG. 2. $G^s(t)$ at 3 different excitation wavelengths in the S_0–S_1 absorption of naphthyl chromophores tagged to polymer chains. $G^s(t)$, which measures the extent of excitation transfer away from the initially excited chromophore, depends on the excitation wavelength, i.e., the transport is dispersive. The sample is a solid mixture of 0.38% by weight 2-VN/MMA copolymers $M_w = 23\,000$, containing 9% 2-VN, in PMMA. (a) The sample temperature is 100 K. There is a pronounced decrease in the decay of $G^s(t)$ as the excitation wavelength is moved to the red. (b) The sample is at room temperature (298 K). $G^s(t)$ still depends on the excitation wavelength, but to a smaller extent than in (a). This demonstrates that the Förster description of donor–donor transport is inadequate to describe the excitation transfer dynamics in this system, even at room temperature.

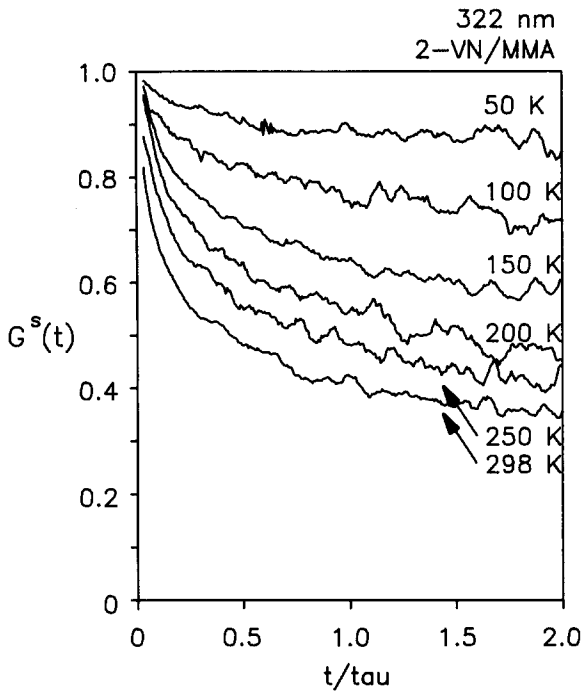

FIG. 3. Temperature dependence of $G^s(t)$ for excitation at 322 nm. The sample is the same as in Fig. 2. Dispersive transport causes $G^s(t)$ to have a dramatic dependence on temperature for excitation on the red edge of the S_0–S_1 absorption. As the temperature is decreased the homogeneous linewidth becomes much smaller than the inhomogeneous broadening. This leaves most neighboring chromophores inaccessible for excitation transfer from a chromophore excited far to the red of the line center.

emission lines render the common low temperature observable unusable at room temperature. At room temperature and near room temperature it has generally been assumed that transport is nondispersive and can be described by the Förster mechanism with appropriate statistical mechanics averaging over the spatial distribution of chromophores. A distribution of site energies has not been considered.

The use of room temperature excitation transport, modeled with the Förster mechanism, is a common tool for the determination of structure and other properties.[3–10] The results presented above provide cause for concern about these measurements. In the following sections a theory is presented which can account for the dispersive transport. In addition, it is shown theoretically and experimentally that there is a magic wavelength at which the effects of dispersive transport vanish from the $G^s(t)$ observable. At the magic wavelength the Förster theory can be used to obtain structural information.

V. THEORY

The problem we wish to address is the calculation $G^s(t)$, the extent of excitation transport vs time, for an ensemble of chromophores with a distribution of site energies. This situation applies to molecules for which the absorption linewidth of an electronic transition has a large contribution from inhomogeneous broadening. Excitation transport between two chromophores with differing transition energies between their ground and excited electronic states requires either absorption or emission of one or more phonons

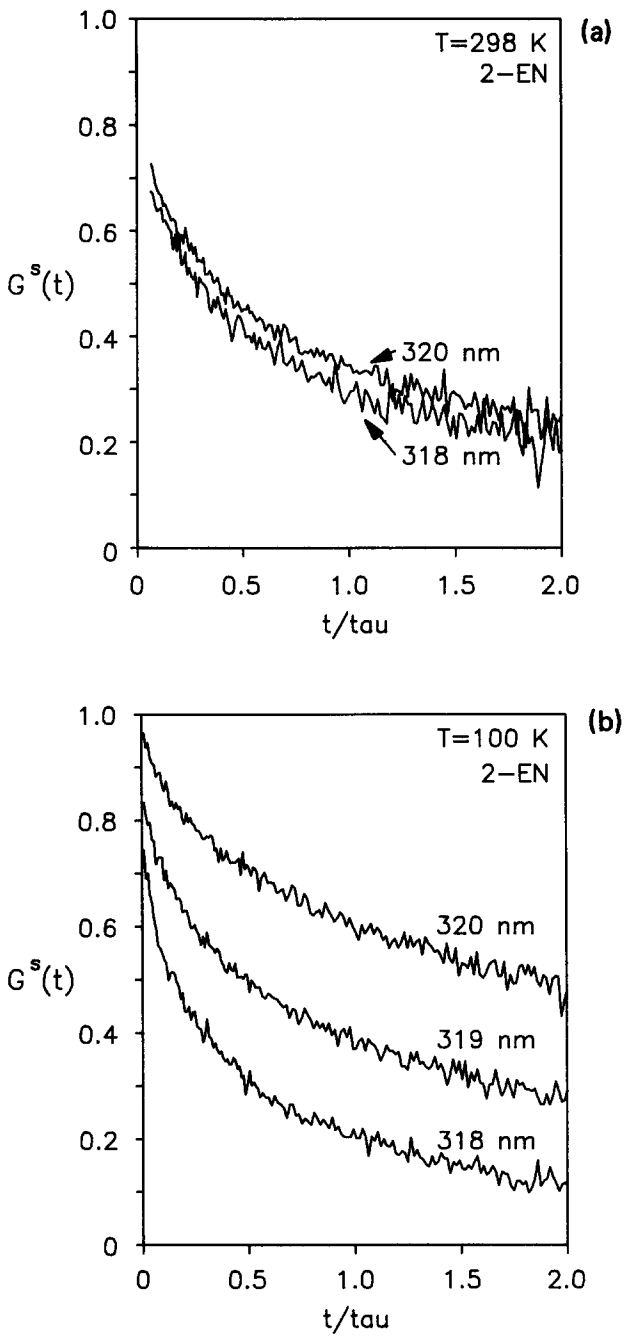

FIG. 4. $G^s(t)$ for 2-ethylnaphthalene (2-EN) randomly distributed in PMMA at different excitation wavelengths. The peak of the S_0–S_1 absorption is at 318 nm for 2-EN in PMMA. The inhomogeneous linewidth is 215 cm^{-1}. The 2-EN dimensionless concentration is $c = 1.2$. $[c = (4/3)\pi R_0^3 \rho]$. (a) $T = 298$ K. The 2-EN chromophores have a narrower distribution of S_0–S_1 transition energies than when the naphthyl chromophores are attached to a polymer chain. Nonetheless, the rate and extent of excitation transfer away from the initially excited chromophore is dispersive; it depends on the laser excitation wavelength. (b) $T = 100$ K.

to conserve energy. The complications in calculating the pairwise transfer rate in situations such as this are due to the need to consider both the interaction of the electronic states of the naphthyl chromophores with the phonon bath and the phonon density of states. Since both of these quantities are difficult to obtain experimentally or theoretically, we have

decided to approach this problem from another angle.

The theory separates the dispersive transport problem into two parts. The first part involves calculating the extent of dispersive transport that occurs in a system under given conditions. This is based on the two limits for an acceptor chromophore. It is either a donor itself, capable of backtransferring an excitation to the initially excited chromophore, or it is a trap, which cannot backtransfer. An effective concentration of chromophores and a scaling factor which accounts for the amount of dispersive transport in the system are calculated. Parameters involved in this calculation include the sample temperature and the inhomogeneous linewidth of the electronic transition. Since, experimentally a distribution of chromophore frequencies are excited initially by the laser light, the calculation is repeated for all possible starting chromophore transition energies.

The second part of the theory uses the results developed in the past for nondispersive electronic excitation transfer.[4,5,32] We combine the modified number density of chromophores available for energy transfer and the dispersive transport parameter calculated in the first part of the calculation, with the theory for nondispersive system of the appropriate chromophore geometry. In this way, the powerful techniques developed over the past years to handle incoherent excitation transfer are applied to the problem of dispersive transport.

Comparisons of the results of the model developed here and the experimental findings demonstrate that, although it ignores the details of individual energy transfer steps, this theory gives near quantitative agreement with experiment. Furthermore, all essential qualitative features of the experimental results are also predicted by the theory.

A brief review of the energy independent incoherent electronic excitation transfer theory will be given here. Then the changes needed to handle the dispersive transport problem will be presented. The quantity of interest is $G^s(t)$, the self part of the Green function solution of the transport master equation. $G^s(t)$ can also be identified with the time-dependent probability that an initially excited chromophore is still excited, independent of lifetime decay. Calculating this quantity theoretically allows direct comparison to the experimental results, in which $G^s(t)$ is the observable.

Recently a mathematically tractable method of calculating $G^s(t)$ for chromophores with complicated geometrical distributions was developed for both donor–donor and donor–trap excitation transfer.[4,5] The theoretical analysis is based on an extension of the first order cumulant expansion method developed by Huber for randomly distributed donors.[31] Donor–donor transfer describes a situation in which the pairwise rate of forward energy transfer, away from the initially excited chromophore to one acceptor chromophore, is equal to the rate of backtransfer from the acceptor. Donor–donor (DD) transfer has two requirements: the donor and acceptor must be energetically equivalent (this usually means they are chemically identical) and the homogeneous broadening of the absorption line must be much greater than the inhomogeneous broadening. Direct trapping, or donor–trap (DT) transfer, occurs in situations in which the backtransfer rate is vanishingly small. Thus, only forward transfer occurs from the donor to the trap. This can occur among any two chromophores whose electronic transition energies differ by an amount greater than the thermal energy that could be absorbed from the host. Direct trapping in complex geometrical systems of chromophores has been described by Baumann and Fayer,[4] who extended Förster's original treatment for a randomly distributed system.

The result for DT is exact. The result for DD is approximate, but it has been shown to be an extremely accurate approximation.[5] Remarkably, the expressions obtained for DD and DT are unified by a scaling factor. Solutions for one spatial arrangement of molecules can be easily extended to either the DD or DT case in this manner.

The expression obtained for the natural logarithm of $G^s(t)$ is,

$$\ln G^s(t) = -\frac{\rho}{\lambda}\int (1 - e^{-\lambda\omega(\mathbf{r})t})u(\mathbf{r})d\mathbf{r}, \tag{5}$$

$\lambda = 1$ for DT,

$\lambda = 2$ for DD.

The two limits of intermolecular excitation transfer differ in the value of the constant λ. $\omega(\mathbf{r})$ is the pairwise transfer rate for two chromophores separated by the three-dimensional vector $\mathbf{r}$, and can be of any form. In the cases considered here this is given by a transition dipole–transition dipole interaction, appropriate for singlet electronic states,

$$\omega(r) = \left|\frac{1}{\tau}\right| \cdot \left|\frac{R_0}{r}\right|^6 \cdot \gamma^2. \tag{6}$$

τ is the excited state lifetime and R_0 is the critical Förster transfer radius.[11] $\lambda = 0.8468$ is a factor which accounts for the static transition dipole orientations of the chromophores in a polymeric glass.[29] $u(\mathbf{r})$ is the chromophore spatial distribution function and ρ is the number density of chromophores.

The analytical solution for a three-dimensional, random, infinite solution of static chromophores is given by[4]

$$\ln G^s(t) = -c\lambda^{-1/2}\gamma\cdot\Gamma\left(\frac{1}{2}\right)\cdot\left(\frac{t}{\tau}\right)^{1/2}. \tag{7}$$

c is the dimensionless concentration,

$$c = \frac{4}{3}\pi R_0^3\rho. \tag{8}$$

This expression for $G^s(t)$ is appropriate for nondispersive transfer in a solid solution of 2-EN in PMMA.

The problem of excitation transport among chromophores tagged to a polymer chain was recently addressed by Peterson and Fayer.[5] Since the chromophores randomly tagged to a polymer chain were chemically identical, DD transfer was considered. However, using Eq. (5) the result can be extended to the problem of one donor and many traps randomly tagged on a chain. The result of the Peterson and Fayer analysis generalized to either DD or DT is given by

$$G^s(t) = \frac{1}{\bar{N}}\sum_{i=1}^{\bar{N}}\exp\left[\frac{1}{\lambda}\int_0^\infty (e^{-\lambda\omega(r)t} - 1)u(\mathbf{r})d\mathbf{r}\right]. \tag{9}$$

In Eq. (9) the exponential term is $G_i^s(t)$, $G^s(t)$ for an excitation started on segment i of a polymer chain of $\bar{N}$ statistical segments. The summation is over all possible starting seg-

ments. In this case $u(\mathbf{r})$ is given by a Gaussian pair-correlation function with a correction term for unexcited chromophores on the same statistical segment as the initially excited chromophore,

$$u(\mathbf{r})d\mathbf{r} = \left\{ np'(r) + \frac{N-n-1}{\bar{N}-1} \sum_{j=1}^{\bar{N}}{}' \left[\frac{3}{2\pi a^2 |i-j|} \right]^{3/2} \times \exp\left[\frac{-3r^2}{2a^2|i-j|} \right] \right\} d\mathbf{r}. \quad (10)$$

$np'(r)$ gives the probability of finding unexcited chromophores on the same chain segment i as the initially excited chromophore. The prime on the summation indicates that $j \neq i$. N is the total number of chromophores tagged to the polymer chain. $\bar{N}$ is the number of statistical segments on the chain and a is the statistical segment length. Provided the molecular weight of the polymer is known, there is one free parameter a. It is directly related to the ensemble averaged root mean square radius of gyration $\langle R_g^2 \rangle^{1/2}$:

$$\langle R_g^2 \rangle = \tfrac{1}{6}\bar{N}a^2. \quad (11)$$

These expressions based on the truncated cumulant expansion were developed for situations in which the pairwise excitation transfer rate $\omega(r)$ is independent of energy difference between chromophores. The inhomogeneous linewidth of the electronic transition is much smaller than the homogeneous linewidth. The extent and rate of excitation transport $G^s(t)$ is independent of the excitation energy in this case; electronic excitation transport is nondispersive.

A method for calculating $G^s(t)$ in the situation of the inhomogeneous and homogeneous linewidths being of comparable magnitude will now be described. In this situation the chemically identical ensemble of acceptor chromophores, spatially near an excited chromophore, has a distribution of electronic transition energies. Because there can be a low probability of having phonons of appropriate energy to make up an energy difference between two spatially near chromophores, this distribution affects an excited chromophores ability to transfer an excitation to a chromophore with a higher S_0–S_1 transition energy. In a sense, the chromophores have a certain probability of being donors, capable of backtransferring the excitation, and a certain probability of being traps relative to the initially excited chromophore.

Consider two chromophores. One has the origin of its S_0–S_1 electronic transition with energy ΔE, the other has transition energy $\Delta E'$. The chromophore with excitation energy ΔE is excited. If $\Delta E'$ is larger than ΔE, a phonon of energy $\Delta E' - \Delta E$, or phonons whose energy add up to this quantity, must be absorbed for the electronic energy to hop to the second chromophore. If this energy difference is small and the temperature of the system is relatively high, the phonons of the appropriate energy will be available. The probability of this absorption occurring is also dependent on the magnitude of the excitation–phonon interaction. If the temperature is relatively low, the energy difference $\Delta E' - \Delta E$ is large, or both, the phonons needed to conserve energy may not be present, and the probability of the excitation being transferred up in energy will be small.

Now consider the case where $\Delta E'$ is smaller than ΔE. Once the excitation has been transferred from the initially excited chromophore to the lower energy chromophore accompanied by phonon emission, the probability of backtransfer occurring depends again on the probability of there being phonons of sufficient energy and on the excitation-phonon coupling.

To rigorously calculate the probability of excitation transfer taking place in the situations discussed above one would need to have a measurement or model for the excitation–phonon coupling and for the phonon density of states. These quantities are difficult to determine. We circumvent the need for these two complicated quantities by considering spectral overlap between homogeneous lines for each chromophore. We assume that each chromophore's electronic transition has homogeneous broadening given by a Lorentzian line shape. For simplicity we will take the full width at half-maximum (FWHM) equal to the thermal energy kT. Then the probability that an electronic excitation on one chromophore, with its transition energy centered at ΔE, can be found on another of higher transition energy $\Delta E'$, independent of spatial separation, is modeled as the spectral overlap of the two Lorentzians:

$$F(\Delta E - \Delta E') = \frac{\int_{-\infty}^{\infty} L(\omega) \cdot L[\omega + (\Delta E - \Delta E')] d\omega}{\int_{-\infty}^{\infty} L(\omega) \cdot L(\omega) d\omega}. \quad (12)$$

$F(\Delta E - \Delta E')$ is the spectral overlap and $L(\omega)$ is a Lorentzian of the form

$$L(\omega) = L_0 \cdot \frac{1}{\omega^2 + (a/2)^2}, \quad (13)$$

where a is the FWHM. This is illustrated in Fig. 5. In this figure the chromophore with S_0–S_1 transition energy ΔE is initially excited, and transfers its excitation to the chromo-

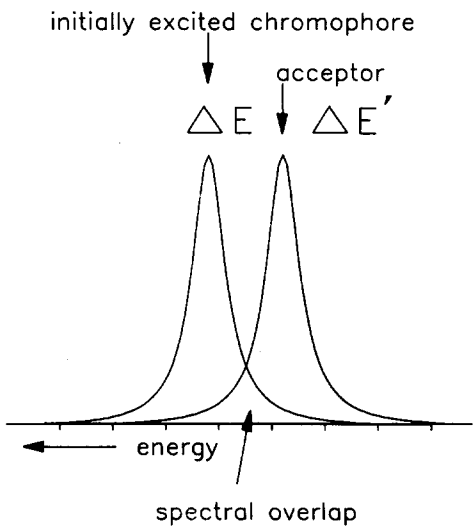

FIG. 5. Illustration of spectral overlap. A chromophore of S_0–S_1 transition energy ΔE has transferred an excitation to a chromophore with a lower transition energy $\Delta E'$. The amount of overlap of the homogeneously broadened chromophore transition energies, modeled as Lorentzian curves, gives the probability that the acceptor at energy $\Delta E'$ can back-transfer the excitation to the chromophore at energy ΔE.

phore with energy $\Delta E'$. The spectral overlap of the two Lorentzian shaped homogeneous lines gives the probability that the excitation can be back-transferred to the originally excited chromophore. The denominator in Eq. (12) normalizes this probability to $F(\Delta E - \Delta E') = 1$ when $\Delta E = \Delta E'$. This is the limit of donor–donor transfer, when the rate of back-transfer between two chromophores is the same as the rate for forward transfer. The donor–trap limit is reached when the quantity $F(\Delta E - \Delta E')$ is zero. Forward transfer to a lower energy chromophore with phonon emission can take place, but backtransfer is impossible.

The spectral overlaps for a chromophore of energy ΔE with chromophores at all transition energies across the inhomogeneous line are calculated using Eq. (12). With a narrow band excitation pulse at energy ω_ϵ, chromophores of all energies have a probability of being excited that is determined by their homogeneous line shape and the energy difference $\Delta E - \omega_\epsilon$. At very low temperature, a narrow region of the inhomogeneous line is excited, and excitation transport occurs with essentially a single starting energy. At or near room temperature there is a broad distribution of initial energies for any given laser frequency. If the inhomogeneous line is modeled as a Gaussian and the homogeneous line as a Lorentzian, the origin of the S_0–S_1 transition has the shape of a convolution of a Gaussian and a Lorentzian. Then the probability of a laser excitation at frequency ω_ϵ exciting a chromophore of energy ΔE is given by

$$N_{\omega_\epsilon}(\Delta E) = \frac{L(\omega_\epsilon - \Delta E)\cdot G(\Delta E)}{\int_0^\infty L(\omega_\epsilon - \Delta E)\cdot G(\Delta E)d(\Delta E)}. \quad (14)$$

$G(\Delta E)$ is a Gaussian centered at ΔE_0 with FWHM a,

$$G(\Delta E) = G_0 \exp\left\{ \frac{-(\Delta E' - \Delta E_0)^2}{a^2\cdot(4\cdot\ln 2)^{-1}} \right\}, \quad (15)$$

and $L(\omega)$ is a Lorentzian, as in Eq. (13). Figure 6 illustrates this for a few possible locations in the model electronic absorption line.

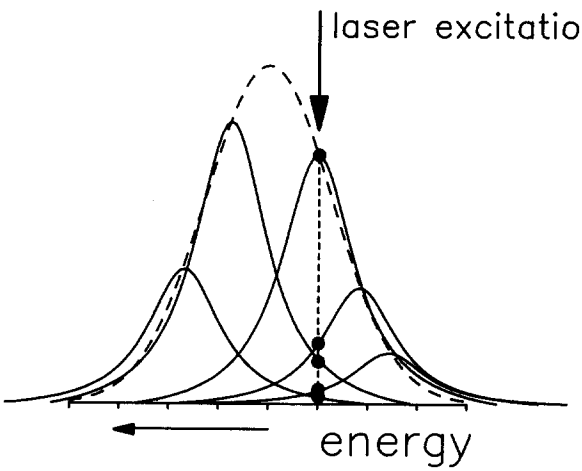

FIG. 6. For excitation at a given frequency in the S_0–S_1 absorption band by a narrow band source, all chromophores have some probability of being excited. This is given by the overlap of the homogeneous line (a Lorentzian curve) centered at the chromophore's S_0–S_1 transition energy with the laser excitation energy [see Eq. (14)]. This is illustrated for a few possible chromophore energies.

The spectral overlap calculation is made for all possible initial excitation energies ΔE to transfer to all possible acceptor energies $\Delta E'$. The fraction of spectral overlap gives the probability that an excitation transfer step is DD, as opposed to DT. Then the fraction of chromophores that can act as donors to the initially excited chromophore, i.e., participate in DD transfer, can be calculated. For example, if the overlap with a particular acceptor is 0.5, that acceptor will give a 0.5 molecule contribution to the number density of donors. This fraction of chromophores for energy $\Delta E'$, lower than the energy of the initially excited chromophore ΔE, is given by,

$$d_r(\Delta E) = \frac{\int_0^{\Delta E} G(\Delta E')\cdot F(\Delta E - \Delta E')d(\Delta E')}{\int_0^{\Delta E} G(\Delta E')d(\Delta E')}. \quad (16)$$

The donor fraction to the blue of ΔE is similarly given by

$$d_b(\Delta E) = \frac{\int_{\Delta E}^\infty G(\Delta E')\cdot F(\Delta E - \Delta E')d(\Delta E')}{\int_{\Delta E}^\infty G(\Delta E')d(\Delta E')}. \quad (17)$$

The Gaussian multipliers in each of these expressions account for the relative density of chromophores that have a given S_0–S_1 transition energy $\Delta E'$. The denominators give $d_r(\Delta E)$ and $d_b(\Delta E)$ ranges of 0 to 1.

The actual number density ρ of chromophores in a sample can be measured experimentally using absorption spectroscopy. With chromophore energies distributed according to a Gaussian profile, the number density to the red of ΔE, ρ_r, and to the blue of ΔE, ρ_b, are given by

$$\begin{aligned} &\left.\begin{aligned}\rho_r(\Delta E) &= [1 - \mathrm{erf}(\Delta E_0 - \Delta E)]\cdot\rho/2\\ \rho_b(\Delta E) &= [1 + \mathrm{erf}(\Delta E_0 - \Delta E)]\cdot\rho/2\end{aligned}\right\} \quad \text{if } \Delta E < \Delta E_0,\\ &\left.\begin{aligned}\rho_b(\Delta E) &= [1 - \mathrm{erf}(\Delta E_0 - \Delta E)]\cdot\rho/2\\ \rho_r(\Delta E) &= [1 + \mathrm{erf}(\Delta E_0 - \Delta E)]\cdot\rho/2\end{aligned}\right\} \quad \text{if } \Delta E > \Delta E_0. \end{aligned} \quad (18)$$

Combining the equations for the donor fractions and the number densities leads to expressions for the number density of chromophores that can act as donors for an excited chromophore of transition energy ΔE, $D(\Delta E)$, and the number density of traps, chromophores than can accept an excitation transfer but cannot backtransfer to the originally excited chromophore $T(\Delta E)$:

$$\begin{aligned} \mathrm{D}(\Delta E) &= d_r(\Delta E)\rho_r(\Delta E) + d_b(\Delta E)\rho_b(\Delta E),\\ \mathrm{T}(\Delta E) &= \rho_r(\Delta E)\cdot[1 - d_r(\Delta E)]. \end{aligned} \quad (19)$$

$\mathrm{D}(\Delta E)$ and $\mathrm{T}(\Delta E)$ do not add up to ρ, the number density. This is because there are chromophores of energy $\Delta E'$, to the blue of ΔE, that have a low probability of accepting an excitation transfer from the initially excited chromophore because of the poor spectral overlap $F(\Delta E - \Delta E')$ for this energy separation. In this theory, these are the chromophores that are inaccessible for excitation transfer from the original chromophore because the necessary phonons to transfer the excitation up in energy are not available due to the temperature of the sample.

What has been done thus far in these calculations is to divide the distribution of chromophores into three types, depending on their electronic transition energies. $D(\Delta E)$ are chromophores which undergo DD transport with the initially excited chromophore. $T(\Delta E)$ is the number density of chromophores which can only accept a transfer of energy; they act as traps for the electronic energy relative to the initially excited chromophore. And finally there are chromophores to the blue of ΔE which cannot, or have a low probability of, accepting an excitation from the initially excited chromophore. The total number density of chromophores which can participate in energy transfer with a chromophore excited by the laser pulse is

$$\rho'\Delta E) = D(\Delta E) + T(\Delta E). \tag{20}$$

Recall from the nondispersive theory outlined above that in the cumulant expansion development of expressions for $G^s(t)$, the DD and DT cases differ only by a factor λ. λ has the limit of 1 for direct trapping and 2 for donor–donor transfer. Using the procedure outlined above the dispersive transport problem has been reduced to a problem of transfer to a mixture of donors and traps. The next step is to adjust λ to model this regime intermediate between all donors and all traps. This will make λ a dispersive transport parameter.

Loring, Anderson, and Fayer (LAF) used an infinite order diagrammatic expansion to the self part of the Green function to develop an accurate expression for $G^s(t)$ for a random solution of donors and traps.[32] To handle the donor and trap problem within the cumulant expansion development of $G^s(t)$, λ is scaled between the limits of $\lambda = 1$ (pure DT) and $\lambda = 2$ (pure DD):

$$\lambda = 1 + \frac{D(\Delta E)}{\rho'}. \tag{21}$$

The linear scaling approach has been compared to the results of the LAF theory for the same concentrations of donors and traps randomly distributed in solution.[27] The agreement between the two theories is very good, demonstrating that the linear scaling of λ provides a simple and accurate method of handling the nondispersive combined donor–donor and donor–trap problem.

The dispersive transport problem has now been reduced to a calculation which can be handled using the cumulant expansion treatment. All the benefits of this technique including the tractable mathematics and the ability to extend the calculation to chromophore distributions more complicated than random can thus be employed in modeling situations in which dispersive transport takes place. $G^s(\Delta E,t)$ is calculated for a chromophore at every energy in the S_0–S_1 absorption line. This involves first calculating the spectral overlap for acceptors at all possible transition energies, determining the number density that can act as donors (with backtransfer) and the number density that can act as traps, and linearly scaling λ between the limits of 1 and 2. The appropriate spatial average over the chromophore distribution function and the starting point of the excitation are taken. $G^s(\Delta E,t)$ is then weighted by the probability that a chromophore at ΔE is excited by the laser pulse with photons of energy ω_ϵ, N_{ω_ϵ}. An integral over all ΔE is taken to arrive at the final observable $G^s(t)$:

$$G^s(t) = \frac{\int_0^\infty G^s(\Delta E,t)\cdot N_{\omega_\epsilon}(\Delta E)d(\Delta E)}{\int_0^\infty N_{\omega_\epsilon}(\Delta E)d(\Delta E)}. \tag{22}$$

Calculating the observable $G^s(t)$ requires doing the integrals over the absorption line numerically.

VI. COMPARISON OF THEORY AND EXPERIMENTS

Figures 7(a) and (b) show data taken at a variety of excitation wavelengths for two temperatures, 150 and 250 K, respectively. The sample is naphthyl tagged PMMA in PMMA host. The smooth lines are calculated using the theory developed in the previous section. There are seven parameters which go into the calculations: (1) the inhomogeneous line center (319.5 nm, 31 298 cm^{-1}), (2) inhomogeneous linewidth (300 cm^{-1}), (3) the critical Förster radius R_0 (13Å), (4) the root mean squared radius of gyration of the tagged polymer chain $\langle R_g^2 \rangle^{1/2}$ (39 Å), (5) the number of chromophores on the tagged chain,[20] (6) the temperature, and (7) the laser excitation wavelength. All of these parameters are known. Therefore the calculated lines in the figures were obtained without adjustable parameters. The effective concentration ρ' and the dispersive transport parameter were calculated as discussed in the previous section. The theory curves have been convolved with a 1 ns instrument response function. This has been measured for the experimental apparatus used here.

While the agreement between theory and experiment is not perfect one can see that the theory predicts the same behavior as is exhibited by the experiment and that the agreement is near-quantitative. To avoid adjustable parameters, we have taken the homogeneous linewidth to be kT. Clearly, the linewidth could be used as an adjustable parameter, which could result in improved agreement. At low temperatures (< 100 K) using kT for the linewidth is a poor approximation.[33] It should be possible to apply this approach at low temperature by independently measuring the homogeneous linewidth using photon echoes or other line narrowing experiments. Another point which should be mentioned in considering the agreement between theory and experiment is the form of the total line shape that was employed. We have used a Voigt profile. However, the S_0–S_1 naphthalene transition sits on the tail of a very strong S_0–S_2 transition. This means that some of the excitation occurs into S_2. Radiationless relaxation then populates an unknown distribution of frequencies in S_1. This was not considered in our calculation. Similarly, an exponential tail of the S_1 absorption to the red, which is caused by hot band absorption, was not included.

The theory shows that decreasing the full width at half-maximum of the Gaussian inhomogeneous line reduces the amount of dispersive transport at any temperature. When the inhomogeneous broadening is smaller the chromophores spatially near an excited chromophore have on average smaller transition energy differences $\Delta E - \Delta E''$, which in turn will lead to an overall greater amount of spectral overlap as given by the overlap function for two Lorentzians.

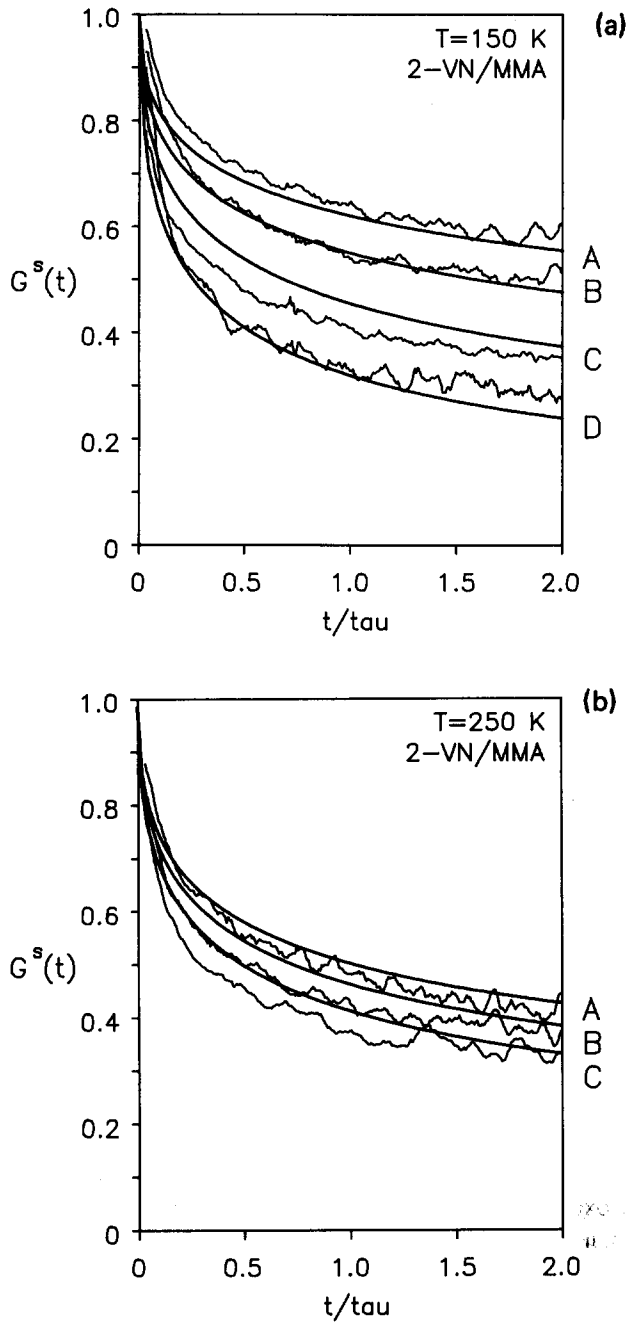

FIG. 7. Comparison of theory and experimental results for dispersive transport for 2-VN/MMA copolymer in PMMA. The parameters used in the calculations were inhomogeneous line center (319.5 nm, 31 298 cm^{-1}), the inhomogeneous line width (300 cm^{-1}), the root mean squared radius of gyration of the polymer chain (39 Å), the critical Förster radius R_0 (13 Å), the number of chromophores on the tagged chains,[20] the temperature, and the laser excitation wavelength. The calculation contains no adjustable parameters. (a) $G^s(t)$ is shown for excitation at (A) 322 nm (31 056 cm^{-1}), (B) 321 nm (31 153 cm^{-1}), (C) 320 nm (31 250 cm^{-1}), and (D) 318 nm (31 446 cm^{-1}). The sample temperature was 150 K. (b) $T = 250$ K. Excitation wavelengths are (A) 322 nm (31 056 cm^{-1}), (B) 321 nm (31 153 cm^{-1}), and (C) 320 nm (31 250 cm^{-1}).

This in turn leads to a greater extent of donor–donor energy transport and a smaller number of inaccessible chromophores at all excitation wavelengths.

As the temperature is lowered there is greater excitation frequency dependence in the energy transport dynamics. This can be seen in Fig. 7. The increased dispersive transport is due to a decrease in the homogeneous linewidth, described by a Lorentzian curve of FWHM equal to the thermal energy of the system (kT). The reduced homogeneous linewidth causes less spectral overlap for the initially excited naphthalene with its neighbors. Thus, the neighboring chromophores are less likely to act as donors, capable of backtransferring the excitation. This increases the likelihood of chromophores to the red acting as traps and reduces the number of chromophores to the blue that are available for energy transfer. The extent to which $G^s(t)$ is affected by this change in temperature depends on the excitation wavelength. When the excitation is on the red side of the absorption line $G^s(t)$ shows a large variation with temperature. This is seen in Fig. 8 for excitation at 322 nm (31 056 cm^{-1}) for the 2-VN/MMA in PMMA system.

We have shown that dispersive excitation transport can and does occur at and near room temperature. We have developed a theoretical description of dispersive transport that is mathematically tractible and permits the inclusion of complex spatial geometries of chromophores. The theory has been compared to experiment and the agreement is quite good. The wavelength dependence of the observable $G^s(t)$ demonstrates that theoretical treatments based on the Förster mechanism are not totally adequate in solid systems, even at room temperature. This can have important ramifications for recent experimental and theoretical work which employ excitation transport to determine complex structures in polymeric solids and other systems. The analysis of data has relied on the Förster transfer mechanism and a detailed statistical mechanical theory which relates the rate of

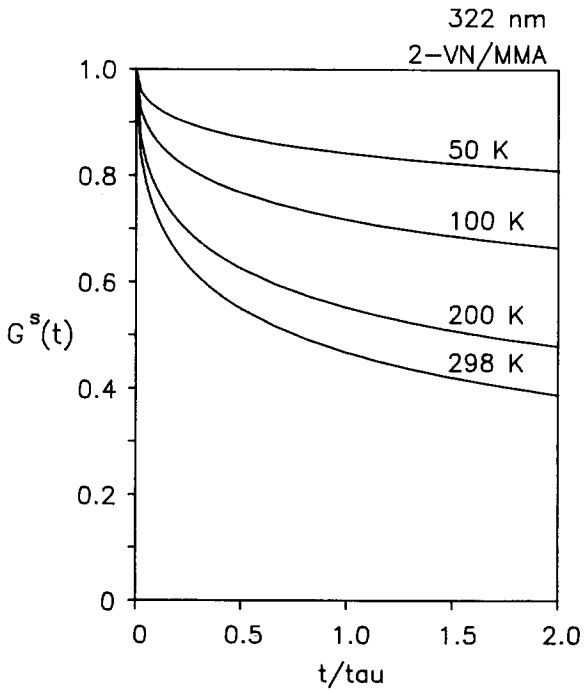

FIG. 8. Calculation of $G^s(t)$ at different temperatures for excitation at 322 nm. Exciting well to the red of the absorption line center results in a dramatic decrease in the extent of excitation transport as the temperature is lowered. The parameters used in the calculations are the same as those for the curves in Fig. 7.

excitation transport to the spatial distribution of chromophores, and therefore the geometrical structure of the system.

It is possible to avoid the complications generated by the existence of dispersive transport by measuring $G^s(t)$ with excitation at a particular wavelength. We call this wavelength the magic wavelength, in analogy to the magic angle at which dipolar interactions can be eliminated from certain experiments. At the magic wavelength, dispersive transport effects vanish from the $G^s(t)$ observable.

It is straightforward to understand qualitatively why a magic wavelength exists. At all temperatures, excitation well to the red side of the inhomogeneous line results in a dispersive transport decay of $G^s(t)$ which is slower than the decay by Förster transport with the same total chromophore concentration. The principal reason is the thermal inaccessibility of a large fraction of the chromophores, resulting in a significant reduction in the effective concentration. Excitation well on the blue side of the inhomogeneous line results in a $G^s(t)$ decay which is substantially faster than the decay by Förster transport. For excitations generated on the blue side of the line most chromophores are traps. There is no backtransfer from a trap. For Förster transfer, all of the chromophores are identical, and the probability of forward and back transfer are identical. Backtransfer slows the decay of $G^s(t)$ by repopulating the initially excited chromophore. If on the red side of the line the dispersive transport $G^s(t)$ decay is slower than that predicted by the Förster theory and on the blue side of the line it is faster than the Förster decay, the dispersive transport $G^s(t)$ must be identical to the Förster decay at some intermediate wavelength.

Figure 9 shows calculations using the full dispersive transport theory of transport among 2-ethylnaphthalene molecules randomly distributed in PMMA. The absorption line center is 318 nm and excitation occurs at 317.3 nm, the magic wavelength for this system. Other measured parameters used in the calculation are the FWHM of the inhomogeneous line (215 cm^{-1}), R_0 (13 Å), and the reduced concentration ($c = 1.2$). The calculations are at three temperatures, 100, 200, and 298 K. The curves are indistinguishable. This is in contrast to Fig. 8, where excitation occurred well to the red of the magic wavelength and the line center. At the magic wavelength $G^s(t)$ does not show a temperature dependence.

The magic wavelength and its significance can be thought of in a different manner. The results of the theory we have developed predict that as the temperature is increased significantly above room temperature, such that kT is much greater than the FWHM of the inhomogeneous line, energy transport will no longer be dispersive. Since the temperature dependence of dispersive transport is removed by exciting at the magic wavelength ω_m, $G^s(t,\omega_\epsilon = \omega_m)$ for any temperature must be equal to $G^s(t,\omega_\epsilon = \omega_m)$ measured at high temperature. This high temperature decay is the nondispersive decay; it is identical to the result of the Förster theory.

Figure 10 shows $G^s(t)$ curves calculated with the Förster theory for randomly distributed 2-EN molecules (solid lines). The figure shows the strong dependence of $G^s(t)$ on the Förster radius R_0. The figure also shows the curve calcu-

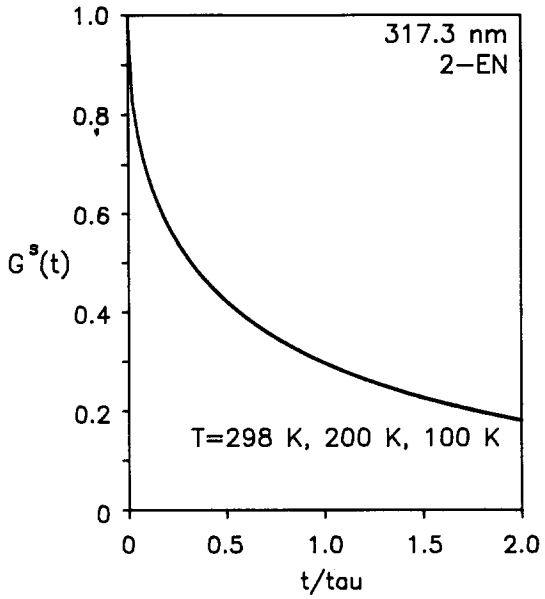

FIG. 9. Calculation of $G^s(t)$ for 2-EN chromophores randomly distributed in PMMA at three different temperatures with excitation at the "magic wavelength." The three curves are identical. Excitation at the magic wavelength removes the temperature dependence of $G^s(t)$, which is a characteristic of dispersive transport (see Fig. 7, for example). The parameters necessary for this calculation are the inhomogeneous line center (318 nm, 31 446 cm^{-1}), the inhomogeneous line width (215 cm^{-1}), R_0 (13 Å), the reduced concentration of chromophores ($c = 1.2$), the temperature, and the excitation wavelength.

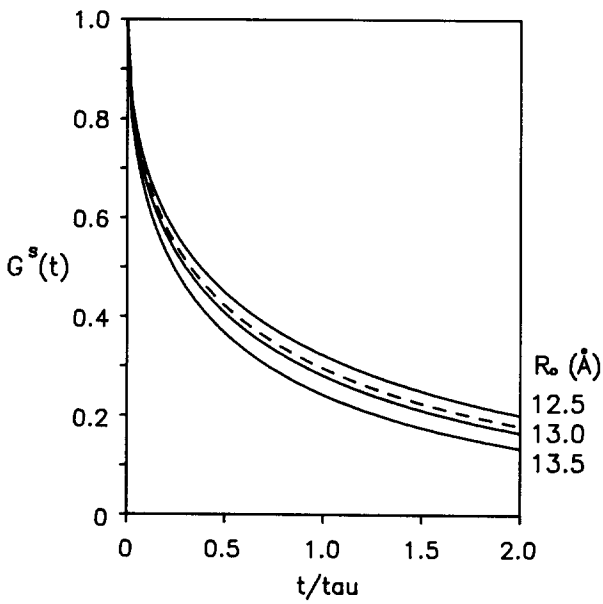

FIG. 10. Comparison of a calculation of $G^s(t)$ at the "magic wavelength" (broken line) with nondispersive calculations at different values of R_0 (solid lines). The nondispersive calculations use the Förster mechanism to describe transport. These three calculations show the sensitivity of $G^s(t)$ to changes in R_0. The calculation for dispersive transport with excitation at the magic wavelength (317.3 nm) and a value of $R_0 = 13$ Å is nearly identical to the Förster result for the same R_0. This shows that this theory which describes dispersive transport predicts that excitation at the magic wavelength gives the same $G^s(t)$ as the Förster theory.

lated with the dispersive transport theory for excitation at the magic wavelength using $R_0 = 13$ Å (dashed line). The magic wavelength curve is almost identical to the $R_0 = 13$ Å curve calculated with the Förster theory. In an actual experiment, noise in the data would make these curves truly indistinguishable. At the magic wavelength, the dispersive transport $G^s(t)$ for a given R_0 is essentially identical in form to the Förster mechanism $G^s(t)$ calculated with the same R_0.

The conclusion is that at the magic wavelength the Förster mechanism will properly describe $G^s(t)$ in spite of dispersive transport. Structural determinations performed at the magic wavelength can be analyzed with models based on the Förster mechanism. It is important to recognize that dispersive transport does not vanish for excitation at the magic wavelength, only the influence of dispersive transport on the observable $G^s(t)$ vanishes. This will not be true for other observables which involve multistep transfer pathways, such as trapping by excimers or other species. Multisteps will move the excitation away from the magic wavelength, and dispersive transport will influence the observables.

We have experimentally searched for the magic wavelength in both the 2-EN in PMMA and the 2-VN/MMA in PMMA mixtures. Both systems exhibit a region of excitation wavelengths over which there is no perceivable temperature dependence in the transport, within experimental noise and error. Figure 11 displays data taken with an excitation wavelength of 319.5 nm on the 2-VN/MMA sample at three temperatures: 298, 200, and 100 K. The data are indistinguishable within the experimental noise. This is in contrast to the data shown in Fig. 3, which was taken on the same sample but with 322 nm as the excitation wavelength. The 322 nm data displays a dramatic change in $G^s(t)$ with temperature. 319.5 nm is the magic wavelength for the 2-VN/MMA in PMMA sample.

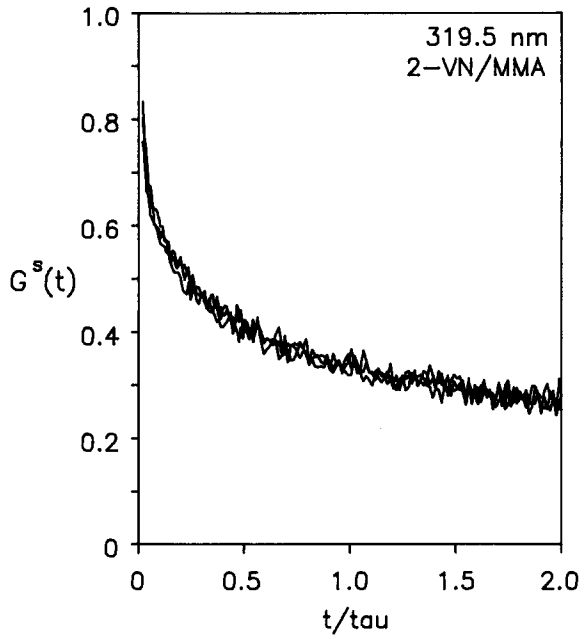

FIG. 11. Experimental results of excitation at 319.5 nm for 2-VN/MMA copolymers in PMMA. The same decay is obtained for three different sample temperatures. 319.5 is the experimentally determined "magic wavelength." This can be compared to Fig. 3, where excitation is far to the red of the magic wavelength, and $G^s(t)$ is strongly dependent on temperature. Excitation at the magic wavelength gives $G^s(t)$ independent of dispersive transport.

Table III gives the absorption line centers for the two samples, 2-EN in PMMA and 2-VN/MMA in PMMA, the calculated magic wavelengths, and the experimentally determined magic wavelengths. The calculated magic wavelengths are about 0.5 nm blue of the line centers. The experimentally determined magic wavelengths are close to the predicted values and virtually at the line centers. Recent structural determinations which used the Förster mechanism in the theoretical analysis of data on 2-VN/MMA samples in PMMA and Poly(vinylacetate) were performed with excitation near the line center.[9,10] Therefore, these experiments should be accurate in spite of the use of the nondispersive transport theory. A complete discussion of the role of dispersive transport in the application of excitation transport to solid state polymer structure determination will be given in another publication.[34]

VII. CONCLUDING REMARKS

Previous experimental and theoretical investigations have addressed the problem of energy-dependent excitation transport dynamics at low temperatures. These studies have almost exclusively investigated systems in which the excitation makes a large number of hops in its lifetime. The experimental observable most often probes those molecules that have received the excitation after a given time. Spectral diffusion is measured. The experimental technique employed in the work reported here is unique in that it probes the initially excited chromophores and measures the probability that they are still excited after a time t, $G^s(t)$. Information on the local environment about the initially excited chromophore is obtained. These measurements of dispersive excitation transport are the first at and near room temperature.

It was shown that the theory presented here exhibits all of the qualitative trends of the dispersive transport measurements. In most cases the agreement is nearly quantitative. This is achieved without resorting to adjustable parameters in the calculations. Many of the ideas incorporated in this theory are simple and idealized. Details such as the phonon density of states and the interaction of the phonons with the electronic state are simplified. However, the close agreement between calculations and experiment demonstrates that the concepts and physical understanding of the effect of dispersive transport are preserved even with the simplifications.

A feature of the approach used here is that dispersive transport is incorporated into previously developed theories for excitation transport among molecules in condensed phase systems. These theories accurately describe the dy-

TABLE III. Results of magic wavelength study.

Sample	S_0–S_1 Line center	Calculated magic λ	Experimental magic λ
2-VN/MMA	319.5 nm	319 nm	319–319.5 nm
2-EN	318 nm	317.3 nm	318–319 nm

namics of an electronic excitation among chromophores in restricted and finite volume geometries. In fact, investigation of the extent of energy transport among chromophores can now be used to obtain quantitative information about the system being studied, such as the radius of micelles, separation of membranes, and ensemble averaged radius of gyration of polymer chains. By accounting for the inhomogeneities in the electronic transition energies of the chromophores when calculating $G^s(t)$, the power of these theories in dealing with the complicated chromophore geometries can be also applied to the problem of dispersive energy transport in systems with complex geometries. In addition, we have shown theoretically and experimentally that a magic wavelength exists. Excitation of the sample at the magic wavelength results in the observable $G^s(t)$ being indistinguishable from that described by nondispersive transport theories, even for systems which display extensive dispersive transport when excited at other wavelengths. Magic wavelength excitation preserves the utility of previous nondispersive transport theories in the determination of structure in complex systems.

ACKNOWLEDGMENTS

This work was supported by the Department of Energy, Office Basic Energy Sciences (DE-FG03-84ER13251). Additional equipment support was provided by the National Science Foundation, Division of Materials Research (DMR 87-18959). We would also like to thank the Stanford Center for Materials Research Polymer Thrust Program for support of this research and for the use of the CMR ps fluorescence instrument used to obtain some of the data. In addition we acknowledge an NSF departmental instrumentation grant (No. CHE 88-21737) which provided computer equipment used in the calculations.

[1] *Molecular Dynamics in Restricted Geometries*, edited by J. Klafter and J. M. Drake (Wiley, New York, 1989); M. D. Ediger and M. D. Fayer, Int. Rev. Phys. Chem. **4**, 207 (1985).
[2] G. H. Fredrickson, H. C. Andersen, and C. W. Frank, Macromolecules **16**, 1456 (1983); **17**, 54 (1984); J. Polym. Sci. Polym. Phys. Ed. **23**, 591 (1985).
[3] M. D. Ediger, R. P. Domingue, and M. D. Fayer, J. Chem. Phys. **80**, 1246 (1984).
[4] J. Baumann and M. D. Fayer, J. Chem. Phys. **85**, 4087 (1986).
[5] K. A. Peterson and M. D. Fayer, J. Chem. Phys. **85**, 4702 (1986).
[6] A. K. Roy and A. Blumen, J. Chem. Phys. **91**, 4353 (1989).
[7] O. Pekcan, M. A. Winnik, and M. D. Croucher, Phys. Rev. Lett. **61**, 641 (1988).
[8] E. Haas, M. Wilchek, E. Katchalski-Katzir, and I. Z. Steinberg, Proc. Natl. Acad. Sci. USA **72**, 1807 (1975).
[9] K. A. Peterson, M. B. Zimmt, S. Linse, R. P. Domingue, and M. D. Fayer, Macromolecules **20**, 168 (1987).
[10] K. A. Peterson, A. D. Stein, and M. D. Fayer, Macromolecules **23**, 111 (1990).
[11] Th. Förster, Ann. Phys. (Leipzig) **2**, 55 (1948); Z. Naturforsch. Teil A **4**, 321 (1949).
[12] K. D. Rockwitz and H. Bässler, Chem. Phys. **70**, 307 (1982); R. Richert and H. Bässler, J. Chem. Phys. **84**, 3567 (1986).
[13] J. R. Morgan and M. A. El-Sayed, J. Phys. Chem. **87**, 383, 2178 (1983).
[14] G. B. Talapatra, D. N. Rao, and P. N. Prasad, J. Phys. Chem. **88**, 4636 (1984); Chem. Phys. **101**, 147 (1986).
[15] R. T. Brundage and W. M. Yen, Phys. Rev. B **34**, 8810 (1986).
[16] M. Harig, R. Charneau, and H. Dubost, Phys. Rev. Lett. **49**, 715 (1982).
[17] H. F. Kauffman, B. Mollay, W. Weixelbaumer, J. Buerbaumer, M. Riegler, E. Meisterhofer, and F. R. Aussenegg, J. Chem. Phys. **85**, 3566 (1986).
[18] E. O. Göbel and W. Grandszus, Phys. Rev. Lett. **48**, 1277 (1982).
[19] T. E. Orlowski and H. Scher, Phys. Rev. Lett. **54**, 220 (1985).
[20] D. L. Huber and W. Y. Ching, Phys. Rev. B. **18**, 5320 (1978).
[21] T. Holstein, S. K. Lyo, and R. Orbach, in *Topics in Applied Physics: Laser Spectroscopy of Solids*, edited by W. M. Yen and P. M. Selzer (Springer, Berlin, 1981), Vol. 49.
[22] P. Avouris, A. Campion, and M. A. El-Sayed, in *Advances in Laser Spectroscopy I* (Society of Photo-Optical Instrumentation Engineers, Bellingham, WA, 1977), Vol. 113.
[23] R. P. Parson and R. Kopelman, J. Chem. Phys. **82**, 3692 (1985).
[24] B. Movaghar, M. Grünewald, B. Ries, H. Bässler, and D. Würtz, Phys. Rev. B **33**, 5545 (1986); M. Grünewald, B. Pohlmann, B. Movaghar, and D. Würtz, Philos. Mag. B **49**, 341 (1984).
[25] S. K. Lyo, Phys. Rev. B **22**, 3616 (1980); G. Schönherr, H. Bässler, and M. Silver, Philos. Mag. B **44**, 47 (1981); R. Richert, B. Ries, and H. Bässler, *ibid.* **49**, L25 (1984).
[26] W. M. Yen and P. M. Selzer, in *Topics in Applied Physics: Laser Spectroscopy of Solids*, edited by W. M. Yen and P. M. Selzer (Springer, Berlin, 1981), Vol. 49.
[27] A. D. Stein, K. A. Peterson, and M. D. Fayer, Chem. Phys. Lett. **161**, 16 (1989).
[28] T. G. Fox, J. B. Kinsinger, H. F. Mason, and E. M. Schuele, Polymer **3**, 71 (1962).
[29] C. R. Gochanour and M. D. Fayer, J. Chem. Phys. **85**, 1989 (1981).
[30] H. Bässler, Phys. Stat. Sol. B **107**, 9 (1981).
[31] W. Y. Ching, D. L. Huber, and B. Barnett, Phys. Rev. B **17**, 5025 (1978); D. L. Huber, D. S. Hamilton, and B. Barnett, *ibid.* **16**, 4642 (1978).
[32] R. F. Loring, H. C. Andersen, and M. D. Fayer, J. Chem. Phys. **76**, 2015 (1982).
[33] M. Berg, C. A. Walsh, L. R. Narasimhan, K. A. Littau, and M. D. Fayer, J. Chem. Phys. **88**, 1564 (1988).
[34] A. D. Stein and M. D. Fayer (to be published).